

Multi-response optimization of crashworthiness parameters of bi-tubular structures

K. Vinayagar* and A. Senthil Kumar^a

Department of Mechanical Engineering, Sethu Institute of Technology, Kariapatti-626115, Tamil Nadu, India

(Received April 10, 2016, Revised November 18 2016, Accepted December 28, 2016)

Abstract. This article aims at presenting multi objective optimization of parameters that affect crashworthiness characteristics of bi-tubular structures using Taguchi method with grey relational analysis. To design the experiments, the L_9 orthogonal array has been used and based on that, the inner tubes have been fabricated by varying the three influence factors such as reference diameter, length difference and numbers of sides of the polygon with three levels, but all the outer cylinders have the same diameter and length 90 mm and 135 mm respectively. Then, the tailor made bi-tubular steel structures were subjected into quasi static axial compression. From the test results it is found that the crushing behaviors of bi-tubular structures with different combinations were fairly significant. The important responses (crashworthiness indicators) specific energy absorption and crush force efficiency have been evaluated from load - displacement curve. Finally optimal levels of parameters were identified using grey relational analysis, and significance of parameters was determined by analysis of variance. The optimum crashworthiness parameters are reference diameter 80 mm, length difference 0 mm and number of sides of polygon is 3, i.e., triangle within the selected nine bi-tube combinations.

Keywords: bi-tubular structures; grey relational analysis; crashworthiness; specific energy absorption; crush force efficiency

1. Introduction

Crashworthy designs of energy absorption structures are very important to minimize the impact of the accidents. At the time of collision, they can absorb maximum kinetic energy by permanent plastic deformation and transfer minimum amount of force to the occupants. The metallic thin-walled tubes are considered as one of the most efficient energy absorbing devices for their easy of manufacture, high strength and low cost. Over the past few decades many of interested scholars studied about crashworthiness of thin walled structures. The analysis of axial loading on thin walled cylinders was pioneered by Alexander (1960) and offered an excellent theoretical model to access average crushing force for axisymmetric fold pattern. Subsequently, Pugsley and Macaulay (1960), Pugsley (1979) and Johnson and Soden (1977) described more about the energy absorption of non-axisymmetric mode. Deformation modes of thin walled cylinders under axial loading were classified by Andrews *et al.* (1983). Abramowicz and Wierzbicki (1989, 1986) analyzed the different types of crushing modes and presented theoretical models by number of experiments on the concertina or ring mode. Hsu and Jones (2004) conducted quasi static and dynamic crushing tests on stainless steel, mild steel and aluminium alloy circular tubes and observed significant difference in deformation force

and energy absorption. Velmurugan and Muralikannan (2009), Alavi Nia and Hamedani (2010) submitted analytical, experimental and numerical results for different cross sectional geometries. To enhance the performance of crashworthiness in thin walled cylinders, researchers used honeycomb or foam as filler materials. Seitzberger *et al.* (2000) and Rajendran *et al.* (2009) studied about the energy absorption capability of foam filled circular tubes and expressed as in thin walled tubes, the fillers can absorbed the energy by plastic deformation and changed collapse mode. Hou *et al.* (2009) resulted in that the foam-filled bitubal structures have more energy absorption capability than the empty and aluminium foam filled tubes. Zhang *et al.* (2012), Yin *et al.* (2011) also used multi objective optimization in honey comb filled single and bi-tubular polygonal tubes, to minimize the Peak Crushing Force (PCF) and maximize the Specific Energy Absorption (SEA). Zhou *et al.* (2011) suggested the use of steel-aluminum hybrid materials can reduce the peak impact force and the total weight, while the total absorbed energy can be greatly increased for the S-shaped front rail, through designing 16 experiments based on orthogonal array by FEA. Hong *et al.* (2014) pointed out increasing the edge length would have faint influence to increase the mean crushing force of triangular lattice tubes. Hong *et al.* (2013) derived the models to predict the mean crushing force of triangular tubes for four different collapse modes. Alavi Nia and Parsapour (2014) explored different configurations in single material and showed that geometric parameter has been a conventional way to improve the crashworthiness of thin walled structures. The effect of length difference in bi-

*Corresponding author, Associate Professor, M.E.,
E-mail: k_vinayagar@ymail.com

^a Professor, Ph.D., E-mail: asenthil123@yahoo.com

tubular structures was reported by Sharifi *et al.* (2015). The influence of different roll angles on crashworthiness of fuselage section was studied by Mou *et al.* (2015). They concluded that the failure modes, deformation, acceleration responses and energy absorption of fuselage section were significantly different when the roll angles changed during the crash.

Although a number of researches and series of achievements have been done by other scholars, they concentrated mainly on single section bi-tubular energy absorbers (same section for inner and outer tubes). In this work, for the first time, the energy absorption capabilities of bi-tubes with two different sections were studied experimentally and Taguchi method with grey relational analysis is used to optimize the multi response such as specific energy absorption and crush force efficiency.

2. Definition of crashworthiness indicators

Total Energy Absorption (EA_{Total}), Specific Energy Absorption (SEA), Average Crush Force (F_{avg}), Peak Crushing Force (F_{max}) and Crush Force Efficiency (CFE) are the important crashworthiness indicators of thin-walled structures which are described with brief explanation.

2.1 Total energy absorption

Total Energy Absorption is equivalent to the mechanical work done by crushing force during the crush distance. It can be calculated as

$$EA_{Total} = \int_0^{\delta} F(\delta)d\delta \quad (1)$$

where $F(\delta)$ is the instantaneous crushing force with a function of the displacement δ . The instantaneous crushing force can be obtained from experiments or numerical modeling.

2.2 Specific energy absorption

Energy absorbed per unit mass of the thin-walled member is known as Specific Energy Absorption

$$SEA = \frac{EA_{Total}}{m} \quad (2)$$

where, m is the mass of the structure. Obviously, a higher SEA indicates a higher energy absorption capability.

2.3 Average crush force

The average crush force is the response parameter for the energy absorption capability

$$F_{avg} = \frac{EA_{Total}}{\delta} \quad (3)$$

where, EA_{Total} is energy absorbed during collapse and displacement (δ).

Table 1 Factors and levels of the experimental process

Factor notation	Factor	Level 1	Level 2	Level 3
		A	Reference Diameter (mm)	60
B	Length difference ($L_i - L_o$)* (mm)	-15	0	15
C	Number of sides of polygon	3	4	6

* L_i = Length of inner tube; L_o = Length of outer tube

2.4 Peak crushing force

Peak crushing force is maximum load in the load-displacement curve usually corresponding to the formation of the first fold. F_{max} is able to determine the occupant's survival rate; therefore, it should be decreased to be close to the mean crushing load as much as possible.

2.5 Crush force efficiency

Crush Force Efficiency is defined as the ratio of the average crush force to the peak crush force.

$$CFE = \frac{F_{avg}}{F_{max}} \times 100 \quad (4)$$

It indicates consistency of load-displacement curve. For the better load consistency, higher CFE value is desirable. If CFE is equal to 100%, that is an ideal crash absorber.

3. Selection and formation of parameters

The most important performance measures in crashworthiness studies are SEA and CFE. In bi-tubular structures they depend on parameters like inner tube reference diameter for determine the edge length of polygon, length difference between inner and outer tubes and number of sides of the polygon. While crushing the bi-tubes with lower diameter difference, the possibility of higher contact between inner and outer tubes may be increased. The sliding of tubes on each other causes a growth in the absorbed energy. Using the tubes with different lengths is a convenient solution to reduce the maximum crushing load since the crushing of both tubes is not coincident (Sharifi *et al.* 2015). The energy absorption capacity increased with the number of section edges. This is due to an increase of the number of folds and plastic hinges in sections with larger number of edges (Alavi Nia *et al.* 2010, 2014). The experiments were conducted with three control factors (reference diameter, length difference and number of sides of the polygon) each at three different levels, and hence, a three level orthogonal array L_9 was selected. The factors and levels of the experimental process are described in Table 1. In setting these parameters, the goal is twofold: maximization of SEA and CFE.

4. Experimental procedure

4.1 Specimen preparation

The specimens were prepared in sheet metal shop from



Fig. 1 Fabrication of specimen by TIG welding

0.478 mm thick ASTM A240 TYPE SS304 stainless steel sheet, since the desirable tube sections were not available in the market. Stainless steel SS304 is considered for its good formability and strength (Rajendran *et al.* 2009). Mechanical properties and chemical composition of this sheet metal were presented in Tables 2-3. The Stainless steel sheet was cut into the required dimensions and jointed by TIG welding which is depicted in Fig. 1. Dimensions and sectional geometry of specimens are shown in Fig. 2. All the outer tubes are circular cylinders with 90 mm diameter and 135 mm length ($L/D = 1.5$). For fabrication of inner tubes edge length, length of the tube and section were taken from Table 4 according to L_9 orthogonal array.

The specimens were coded for easy identification and evaluation. For each type, three samples (9×3) were fabricated and designated as 1-1, 1-2 and 1-3 describe the first, second and third sample of particular item 1 as shown in Fig. 3.

4.2 Experimental process

For this analysis, quasi static axial crushing of samples carried out at a loading rate of 10 mm/min. on servo controlled universal testing machine (FSA make, Model TUF-CN 1000, Fig. 4). In the axial compression, no fixture was used to hold the specimens in place between movable lower table and fixed upper cross-head. Concentric circles drawn in a paper and centre of the concentric circles was coincided with the centre of the movable lower table as shown in Fig. 5 ensure that the axis of the inner and outer tubes was exactly in line with the axis of the machine. The

Table 2 Mechanical properties of SS304-stainless steel sheet

Property	Tensile strength (MPa)	Yield stress (MPa)	% of Elongation
Value	650.32	410.19	41

Table 3 Chemical composition (in wt%) of SS304-stainless steel sheet

Composition	C	Mn	Si	S	P	Ni	Cr	Fe
wt%	0.066	0.950	0.260	0.005	0.037	8.010	18.18	Bal.

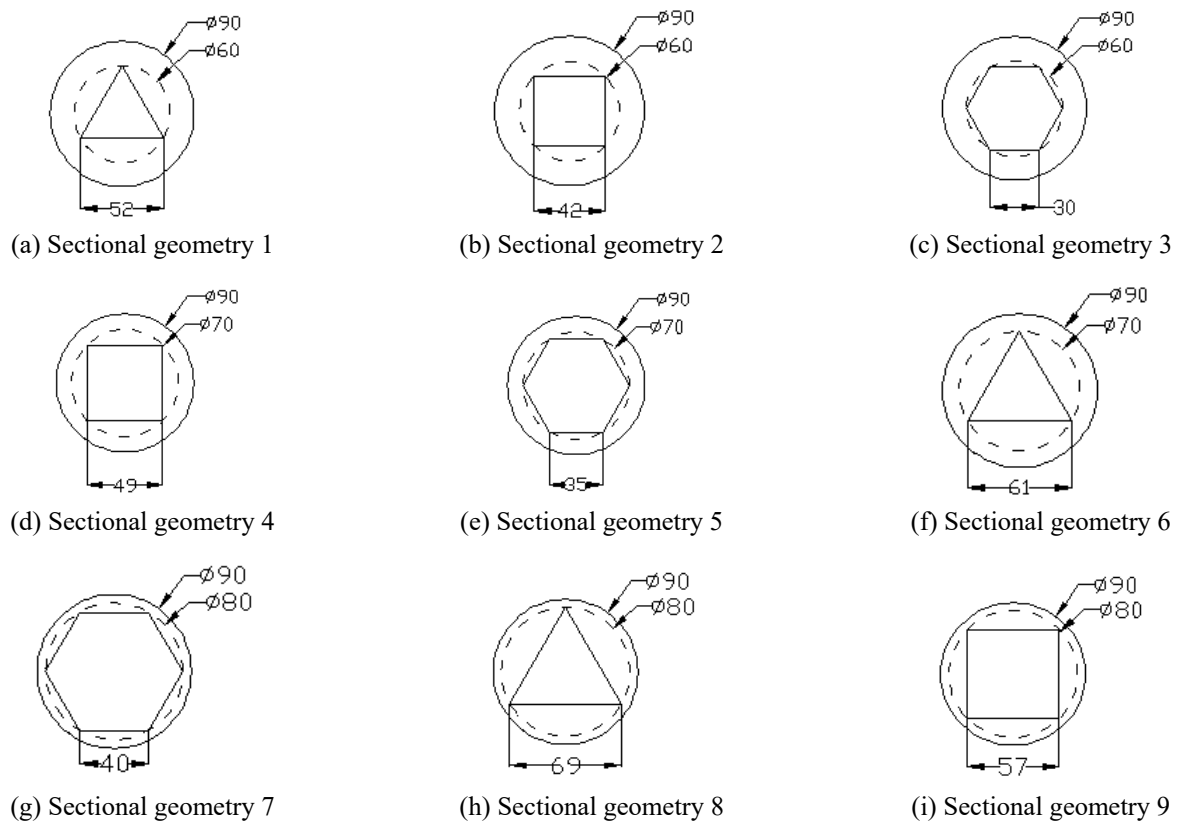


Fig. 2 Dimensions and sectional geometry of specimens for the tests 1 to 9 (All dimensions are in mm)

Table 4 Experimental Layout using L_9 Orthogonal array with coded and original level values

Test number	Parameters / Factors for inner tubes								
	Reference diameter (mm) A		Edge length (mm)	Length difference ($L_i - L_o$) (mm) B		Length (mm)	Number of sides of polygon C		Section
	Coded value	Original value		Coded value	Original value		Coded value	Original value	
1.	1	60	52	1	-15	120	1	3	Triangle
2.	1	60	42	2	0	135	2	4	Square
3.	1	60	30	3	15	150	3	6	Hexagon
4.	2	70	49	1	-15	120	2	4	Square
5.	2	70	35	2	0	135	3	6	Hexagon
6.	2	70	61	3	15	150	1	3	Triangle
7.	3	80	40	1	-15	120	3	6	Hexagon
8.	3	80	69	2	0	135	1	3	Triangle
9.	3	80	57	3	15	150	2	4	Square



(a)



(b)



(c)



(d)



(e)



(f)



(g)



(h)



(i)

Fig. 3 Fabricated specimens before loading for the test 1 to 9



Fig. 4 Servo controlled Universal Testing Machine



Fig. 5 Co-axial positioning of inner tube

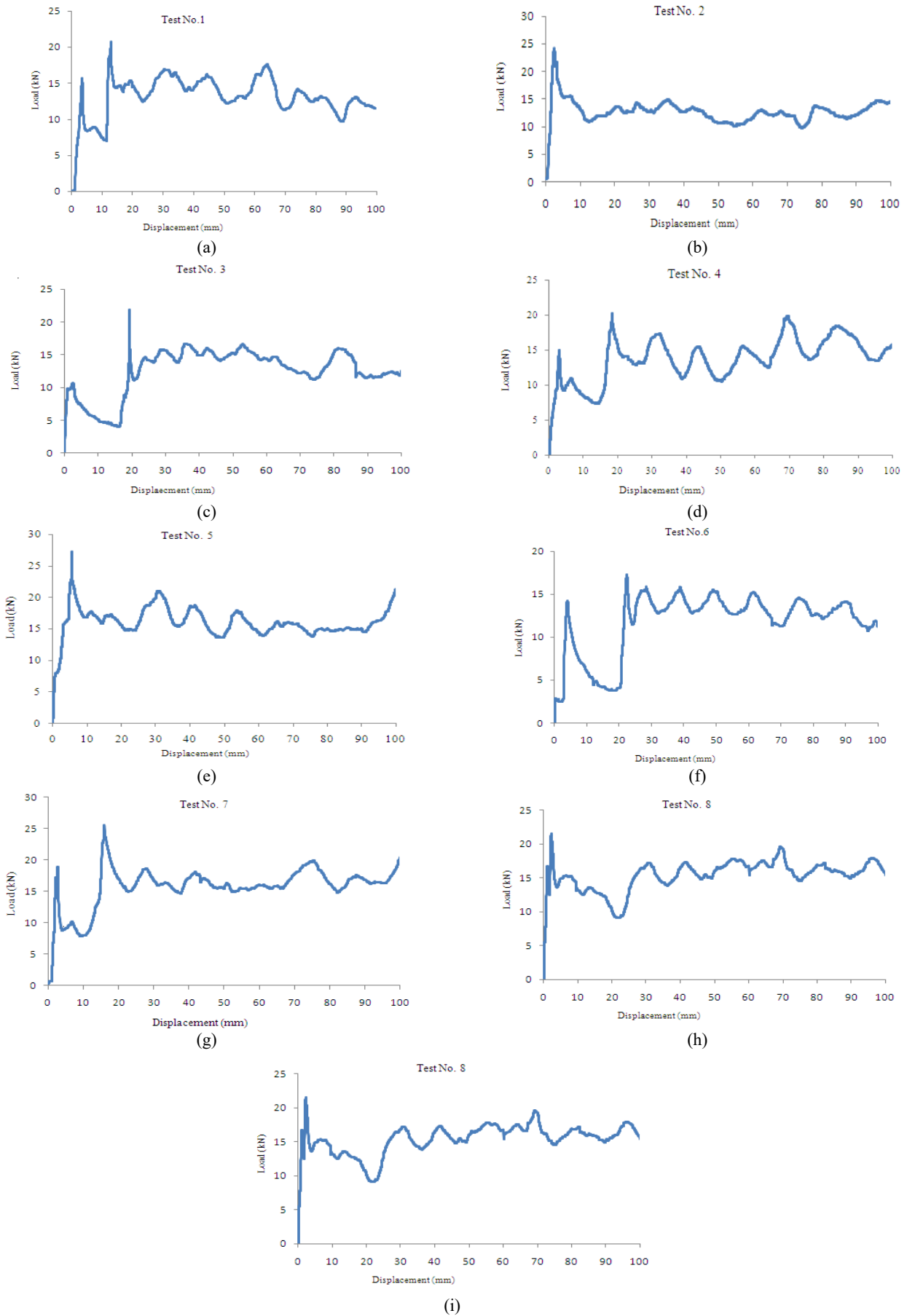


Fig. 6 Load–displacement curves of test 1 to 9

Table 5 Output values of experiments

Test No.	Mass (kg)	F_{max} (kN)	F_{avg} (kN)	EA_{Total} (J)	SEA (kJ/kg)	CFE (%)
1.	0.210	20.70	13.11	1311.2	6.24381	63.33
2.	0.223	24.12	12.66	1271.5	5.70154	52.49
3.	0.239	21.91	12.08	1205.8	5.04512	55.11
4.	0.228	20.22	13.49	1353.6	5.93684	66.72
5.	0.243	27.25	16.77	1598.1	6.57657	61.54
6.	0.245	17.27	11.76	1177.1	4.80449	68.09
7.	0.247	25.46	16.16	1616.6	6.54484	63.46
8.	0.245	21.50	15.40	1540.3	6.28671	71.61
9.	0.267	23.79	14.23	1420.9	5.32181	59.83

specimens were crushed up to 100 mm at the room temperature of 25°C. For each type of geometry, tests are repeated three times and the average values of the main indicators are calculated from the load–displacement curves of the specimens and recorded in Table 5. Furthermore, load–displacement curves for quasi static tests are exposed in Fig. 6.

5. Results and discussion

5.1 Discussion on experimental results

All the load displacement curves have two peak loads except tests 2, 5, and 8. The first peak load indicates the folding of longer tube and then the shorter tube takes the load with longer tube. Hence the second is higher than the first peak load. It is clearly shown in Fig. 6. The second peak load is used for crashworthiness performance calculations. The load displacement curves for the tests 2, 5 and 8 have only one peak load because the inner and outer tubes have same length, and the crushing of both tubes is coincident. While crushing, diamond mode is observed in all bi-tubes. From the experimental results, the effect of inner tube reference diameter, length difference and number of sides of polygon on crashworthiness performance are analyzed.

5.1.1 Effect of reference diameter

By keeping the dimensions of outer cylinder as constant, the effect of changing the inner tube reference diameter on crashworthiness is studied. If inner tube reference diameter

increased from 60 mm to 80 mm consequently the edge length of inner tube polygon was increased; it leads to improve the energy absorption capability (Hong *et al.* 2014). While crushing the lower diameter difference, increase the possibility of higher contact between inner and outer tubes. The sliding of tubes on each other causes a growth in the absorbed energy (Sharifi *et al.* 2015). From Table 5, generally EA_{Total} of specimens increased with inner tube reference diameter. EA_{Total} for reference diameter 60 mm is low, 70 mm is medium and 80 mm is high.

Fig. 7 shows the folding pattern of bi-tubes for the square sectional inner tube combinations in all the three reference diameters. (test 2, test 4 and test 9). In external tube the number of folds increased and length of fold decreased with increasing of reference diameters. Increasing of reference diameters may change the folding pattern of the polygonal edges as well as outer tube and is also one of the reasons for improvement of the energy absorption.

5.1.2 Effect of length difference

The high value of average peak load was obtained at level 2 of length difference in all levels of inner tube reference diameters and number of sides of polygon, because at this level there is no length difference between the tubes. It affects the crush force efficiency of bi-tubular structures. Using the tubes with different lengths in bi-tubular structures is one way of solution to reduce the peak load (Sharifi *et al.* 2015). In level 1, and 3, the tubes have length difference hence their average peak load was significantly low when compared to level 2. This is the desirable factor to improve the CFE. In tests 1, 4 and 7 the outer cylinder takes the load first but in tests 3, 6 and 9 the inner polygonal section tubes receive the load first. The first peak load of tests 1, 4 and 7 is comparatively higher than the test 3, 6 and 9. It can be seen that the outer circular tubes may receive the load in a more stable manner than the inner polygonal tubes (Alavi Nia *et al.* 2010, Velmurugan and Muralikannan 2009).

The effect of length difference on crushing modes is negligible and it plays a major role to reduce the peak load and increase the CFE.

5.1.3 Effect of number of sides of polygon

Number of sides of polygon is also another one important parameter for energy absorption. Number of plastic hinges and folds are increased with number of sides of polygon (Alavi Nia *et al.* 2010). That is the main reason for improvement of energy absorption capacity. Maximum energy absorption EA_{Total} 1616.6 J was obtained in the test

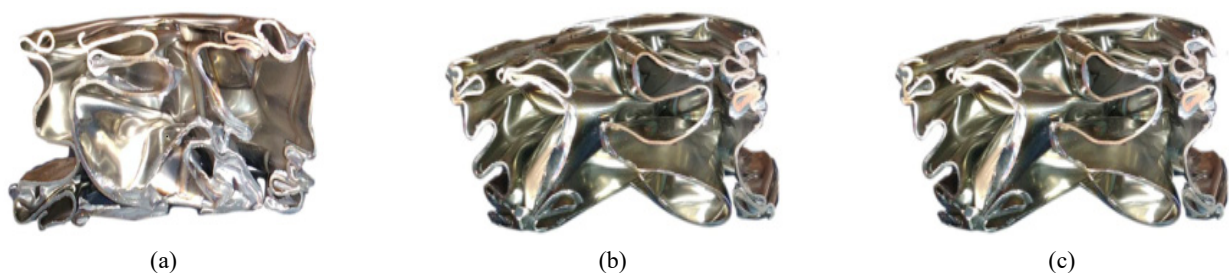


Fig. 7 Folding style of the specimen: (a) test 2; (b) test 4; and (c) test 9

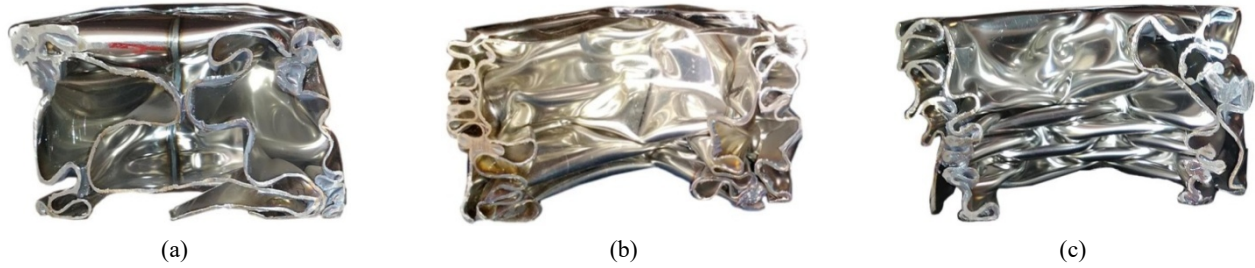


Fig. 8 Folding style of the specimen (a) test 8; (b) test 9; and (c) test 7

no. 7, because it has less diameter difference and higher number of sides of polygon 6 i.e., hexagon. In SEA point of view hexagonal tubes (Test no. 3, 5, 7) dominates the others, maximum value of SEA 6.57657 kJ/kg was recorded in test no. 5 with the parameters combination of inner tube reference diameter 70 mm, Length difference 0 mm and No. of sides of polygon 6 and also it has maximum value of peak load as 27.25 N. Because of their higher peak load, the bi-tubes with hexagonal inner tube combinations have less CFE. The triangular tubes (Test no. 1, 6, 8) have less peak load than the other combination of tubes. So they have maximum value of CFE. Test no.8 (Inner tube reference diameter 80 mm, Length difference 0 mm and No. of sides of polygon 3) has highest value of CFE as 71.61%.

The folding patterns of bi-tubes for triangular, square and hexagonal sections with the reference diameter of 80 mm are shown in Fig. 8 ((a) test 8; (b) test 9; and (c) test 7). The number of folds is increased simultaneously the length of fold decreased for the increasing of sides of the polygon. It leads to change the folding pattern of outer tubes. In triangular inner tube (Test 8), have less number of folds and length of fold is more compared to square (Test 9). The hexagonal section (Test 7) has more number of folds and length of fold is less than the square section.

Though the bi-tubular structures are unequal in size, shape and length, the structures are compared in Table 6 by Specific Energy Absorption (SEA) and Crush Force Efficiency (CFE). Based on minimum mass, the test 1 was taken as base test for this assessment. From Table 6, the percentage of change in SEA is decreased in test 2, 3, 4, 6 and 9 and it is increased in test no. 5, 7 and 8. Test 5 has

Table 6 Comparison with base test No.1

Test No.	Mass (kg)	SEA (kJ/kg)	CFE (%)	% change in SEA	% change in CFE	% increase in mass
1 (BASE)	0.21	6.244	63.33	0	0	0
2	0.223	5.702	52.49	↓8.685	↓17.117	6.191
3	0.239	5.045	55.11	↓19.198	↓12.979	13.809
4	0.228	5.937	66.72	↓4.916	↑5.353	8.571
5	0.243	6.577	61.54	↑5.329	↓2.826	15.714
6	0.245	4.805	68.09	↓23.052	↑7.516	16.667
7	0.247	6.545	63.46	↑4.821	↑0.205	17.619
8	0.245	6.286	71.61	↑0.687	↑13.074	16.667
9	0.267	5.322	59.83	↓14.767	↓5.527	27.143

the highest value of percentage improvement in SEA, but its CFE is only 61.54% which is 2.826% less than the base test 1. If this combination is adopted in vehicle, it will cause the serious harm to the passengers because of its high peak load. When compared to base test 1, the percentage of change in CFE is less in tests 2, 3, 5 and 9 and more in tests 4, 6, 7 and 8. Considering the overall improvements in both SEA and CFE, the test 7 and 8 has better performance compared to the other combinations. Between test 7 and 8, the test 8 has less percentage increase in mass than test 7. Especially the test 8 can improve the CFE by 13.074% and SEA by 0.687% compared to the base test 1.

5.1.4 Theoretical predictions

The test 8 has best combination of bi-tubes i.e., circular and triangular tubes. So the theoretical predictions are derived for that test. To predict the mean crushing force, there are several theoretical models have been addressed by many researchers for concertina and diamond mode of circular tubes. The important expressions of mean crushing force for diamond mode was derived by Pugsley and Macaulay (1960) is

$$F_{avg} = \sigma_o \pi (10t^2 + 0.13Dt) \quad (5)$$

for triangular tube Hong *et al.* (2013) presented a model for the mean crushing force is

$$F_{avg} = 26.66M_o \left(\frac{c}{t} \right)^{\frac{1}{3}} \quad (6)$$

where, $M_o = \sigma_o t^2/4$, σ_o is the flow stress, t is the thickness and D is the diameter of the cylinder and c is the side of triangular tubes. Eqs. (5) and (6) are used to predict the mean crushing force of test no. 8 in the experiment. Since diamond mode is developed in test no. 8

$$\sigma_o = \frac{2}{\sqrt{3}} \sigma_u \quad (7)$$

The predicted mean crush force for circular tube is 11.72 kN and for triangular tube is 3.78 kN with Eqs. (5) and (6) respectively. The addition of these two mean forces is 15.5 kN which is good agreement with the experimental (test 8) mean crush force 15.4 kN.

5.2 Discussion on optimization results

5.2.1 Taguchi method

Table 7 S/N ratio, normalized S/N ratio, Grey relational coefficient, Grey relational grade and its rank

Test No.	Response I (SEA)			Response II (CFE)			Grey relational grade	Rank
	S/N ratio	Normalized S/N ratio	Grey relational coefficient	S/N ratio	Normalized S/N ratio	Grey relational coefficient		
1.	15.90899	0.8346211	0.751	36.0321897	0.60440821	0.558	0.655	4
2.	15.11999	0.5452975	0.524	34.4015314	0	0.333	0.428	8
3.	14.05743	0.1556572	0.372	34.8246082	0.15681462	0.372	0.372	9
4.	15.47110	0.6740491	0.605	36.4851207	0.77228839	0.687	0.646	5
5.	16.35998	1	1.000	35.7831498	0.51210084	0.506	0.753	3
6.	13.63294	0	0.333	36.6616666	0.83772564	0.755	0.544	6
7.	16.31798	0.9845956	0.970	36.0500013	0.61101013	0.562	0.766	2
8.	15.96846	0.8564304	0.777	37.0994734	1	1.000	0.888	1
9.	14.52118	0.3257159	0.426	35.5383800	0.42137621	0.463	0.445	7

* Total mean grey relational grade = 0.611

To obtain the optimum set of parameters, multi objective optimization method grey relational analysis is used in this analysis. Taguchi method is a quality analysis to evaluate the results obtained from the experiments. In any crash-worthiness studies, the main objective is to maximize SEA and CFE. The Higher the Better (HB) type Signal-to-Noise (S/N) ratio was calculated from the following equation

$$S/N \text{ Ratio} = -10 \log_{10} \left(\frac{1}{j} \right) \sum_{i=1}^j \frac{1}{y_i^2} \quad (8)$$

where

- j = number of repetitions of the experiment and
- y_i = observed response value.

5.2.2 Grey relational analysis

First step of the grey relational analysis is all the experimental data have been normalized in the range from zero to one. The normalized result of HB was obtained from the following equation

$$x_i(k) = \left(\frac{\eta_i(k) - \min \eta_i(k)}{\max \eta_i(k) - \min \eta_i(k)} \right) \quad (9)$$

where

- $k = 1$ to n , $i = 1$ to 9 , n is performance characteristic and i is trial number.

After calculating normalized values, the grey relational coefficient $\zeta_i(k)$ can be calculated as

$$\zeta_i(k) = \left(\frac{\Delta_{\min} + \psi \Delta_{\max}}{\Delta_{0i}(k) + \psi \Delta_{\max}} \right) \quad (10)$$

where

$$\Delta_{0i} = \|x_0(k) - x_i(k)\|$$

Difference of the absolute value $x_0(k)$ and $x_i(k)$

$$\Delta_{\min} = \min_{\forall j \in i} \min_{\forall k} \|x_0(k) - x_j(k)\|$$

Smallest value of Δ_{0i}

$$\Delta_{\max} = \max_{\forall j \in i} \max_{\forall k} \|x_0(k) - x_j(k)\|$$

Largest value of Δ_{0i}

Ψ is distinguishing coefficient and its widely accepted

value is 0.5.

Finally averaging the grey relational coefficients, the grey relational grade γ_i can be obtained as

$$\gamma_i = \left(\frac{1}{n} \sum_{k=1}^n \zeta_i(k) \right) \quad (11)$$

where,

n = number of performance characteristics.

The values of S/N ratio, normalized S/N ratio, grey relational coefficient, grey relational grade calculated from the above equations (Eqs. (8) to (11)) tabulated in Table 7. From Table 7, experiment 8 the combination of inner tube reference diameter 80 mm, length difference 0 mm and number of sides of polygon is 3 (triangle) has the highest grey relational grade. The higher the grey relational grade, the better will be the multi performance characteristics. Therefore, the experiment 8 has the optimal parameters setting for the best multi-performance characteristics such as SEA and CFE within the above taken nine combinations.

Fig. 9 shows the response graph of the average grey relational grade for each level of the parameters. Based on the higher grey relation grade optimum level of each controllable factor was determined. The average grey relation grade and the optimum levels of process parameters combination was obtained from Table 8, i.e., optimal inner

Table 8 Response of average grey relational grade

Factor notation	Control factor	Average grey relational grade by factor level			Max-Min
		Level 1	Level 2	Level 3	
A	Reference diameter (mm)	0.485	0.648	0.700*	0.215
B	Length difference ($L_i - L_o$) (mm)	0.689	0.690*	0.454	0.236
C	Number of sides of polygon	0.696*	0.506	0.630	0.190

* Indicates optimum level of factors

A3 B2 C1. This optimized factor levels combination

Table 9 Results of ANOVA

Factor notation	Control factor	Dof	Sum of squares	Mean squares	F value	% Contribution
A	Reference diameter (mm)	2	0.075	0.038	19*	30.36
B	Length Difference ($L_i - L_o$) (mm)	2	0.111	0.056	28*	44.94
C	Number of sides of polygon	2	0.056	0.028	14	22.68
E	Error	2	0.005	0.002		2.02
Total		8	0.247	0.124	#	100.00

* Significant at 95% confidence level

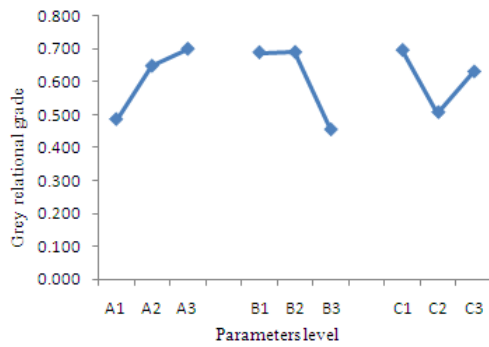


Fig. 9 Response graph of average grey relational grade

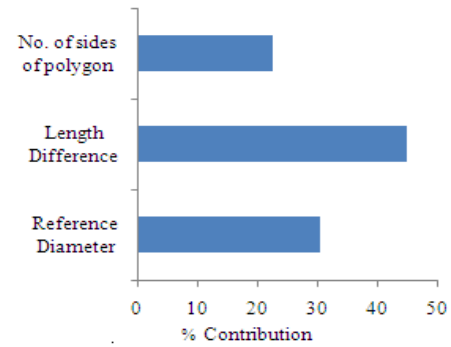


Fig. 10 Percentage contribution for SEA and CFE

inner tube reference diameter, level 3; optimal length difference, level 2; optimal number of sides of polygon, level 1; and the optimal process parameters combination, A3 B2 C1. The values of the optimum process parameters are inner tube reference diameter 80mm, length difference 0mm and number of sides of polygon 3, i.e., triangle.

The difference between the maximum and the minimum value (Max–Min) of the grey relational grade is also indicated in Table 8. The maximum of Max–Min value is the most effective factor affecting the multi-performance characteristics. The maximum of the Max–Min value is 0.236, and the corresponding control factor, length difference has the strongest effect on multi-performance characteristics. The order of importance of the controllable factors can be listed as: factor B (length difference), factor A (reference diameter) and factor C (number of sides of polygon), i.e. $0.236 > 0.215 > 0.190$. Factor B is the most controllable factor in the crashworthiness studies for the multi-performance characteristics.

The significance of the process parameters was tested by ANOVA. Using grey relational grade value, ANOVA was formulated for identifying the significant factors. The results of ANOVA are presented in Table 9 with Fig. 10. In this investigation, length difference between inner and outer tubes (44.96%) was found most significant factor and played a major role followed by inner tube reference diameter (30.36%) and number of sides of inner polygon (22.68%).

5.3 Predicted optimum condition

The optimum level of parameters setting was found as

already exists within the designed experiments as Test No. 8, for this reason it is not necessary to run the confirmation test. The predicted grey relational grade using optimum crashworthiness parameter can be expressed as

$$\hat{\gamma} = \left(\gamma_m + \sum_{i=1}^q (\bar{\gamma}_i - \gamma_m) \right) \quad (12)$$

where,

- γ_m The total mean grey relational grade
- $\bar{\gamma}_i$ The mean grey relational grade at the optimum level
- q Number of parameters that significantly affect the SEA and CFE

The predicted value of grey relation grade, obtained from Eq. (12) is 0.864; whereas the existing grey relation grade value at the optimum condition experiment No. 8 (A3 B2 C1) is 0.888. Hence the difference is only 0.024 i.e., 3% (approx.). This variation occurs due to neglecting the nonlinear effects in three factor three level Taguchi L_9 orthogonal array.

6. Conclusions

This analysis presents the effect of inner tube reference diameter, length difference between the tubes and number of sides of the polygon on crashworthiness capability of bi-tubular structures. After first peak load, the load taken by longer tube is reduced into below the average load F_{ave} . It is caused by more length difference. Reduction in length difference will help to improve the average load. The hexagonal inner tube combinations have higher EA_{Total} and

SEA, at the same time, they have high value of peak load which is undesirable one. The suitable crush initiators can reduce the peak load of these structures.

Based on grey relational approach the following conclusions can be made.

- The optimum process parameters are reference diameter 80 mm, length difference 0 mm and number of sides of polygon is 3, i.e., triangle.
- The order of importance of the factor is as follows: length difference, reference diameter, and number of sides of polygon respectively.
- The largest max–min value of grey relational grade was found from the response table. These values clearly pointed out that the length difference between inner and outer tubes is the predominant factor among the others.
- It insists, need of more investigations on the effect of length difference between inner and outer tubes to improve the crashworthiness capability.
- Experimental analysis described in this work would be useful in the development process of bitubular energy absorption structural components in the field of aircraft, marine and automobile applications.

References

- Abramowicz, W. and Jones, N. (1986), “Dynamic progressive buckling of circular and square tubes”, *Int. J. Impact Eng.*, **4**(4), 243-270.
- Abramowicz, W. and Wierzbicki, T. (1989), “Axial crushing of multi corner sheet metal columns”, *J. Appl. Mech.*, **56**(1), 113-120.
- Alavi Nia, A. and Hamedani, J.H. (2010), “Comparative analysis of energy absorption and deformations of thin walled tubes with various section geometries extrusions”, *Thin-Wall. Struct.*, **48** (12), 946-954.
- Alavi Nia, A. and Parsapour, M. (2014), “Comparative analysis of energy absorption capacity of simple and multi-cell thin-walled tubes with triangular, square, hexagonal and octagonal sections”, *Thin-Wall. Struct.*, **74**, 155-165.
- Alexander, J.M. (1960), “An approximate analysis of the collapse of thin cylindrical shells under axial loading”, *Q. J. Mech. Appl. Math.*, **13**(1), 10-15.
- Andrews, K.R.F., England, G.L. and Ghani, E. (1983), “Classification of the axial collapse of cylindrical tubes under quasi-static loading”, *Int. J. Mech. Sci.*, **25**(9-10), 687-696.
- Hong, W., Jin, F., Zhou, J., Xia, Z., Xu, Z., Yang, L., Zheng, Q. and Fan, H. (2013), “Quasi-static axial compression of triangular steel tubes”, *Thin-Wall. Struct.*, **62**, 10-17.
- Hong, W., Fan, H., Xia, Z., Jin, F., Zhou, Q. and Fang, D. (2014), “Axial crushing behaviors of multi-cell tubes with triangular lattices”, *Int. J. Impact Eng.*, **63**, 106-117.
- Hou, S., Li, Q., Long, S., Yang, X. and Li, W. (2009), “Crash worthiness design for foam filled thin – wall structures”, *Mater. Des.*, **30**(6), 2024-2032.
- Hsu, S.S. and Jones, N. (2004), “Quasi-static and dynamic axial crushing of thin-walled circular stainless steel, mild steel and aluminium alloy tubes”, *Int. J. Crash Worthiness*, **9**(2), 195-217.
- Johnson, W. and Soden, P.D. (1977), “In extensional collapse of thin-walled tubes under axial compression”, *J. Strain Anal.*, **12**(4), 317-330.
- Mou, H., Du, Y. and Zou, T. (2015), “Effects of different roll angles on civil aircraft fuselage crashworthiness”, *Adv. Aircraft Spacecraft Sci.*, **2**(4), 391-401.
- Pugsley, A.G. (1979), “On the crumpling of thin tubular structures”, *Q. J. Mech. Appl. Math.*, **32**(1), 1-7.
- Pugsley, S.A. and Macaulay, M. (1960), “The large-scale crumpling of thin cylindrical columns”, *Q. J. Appl. Math.*, **13**(1), 1-9.
- Rajendran, R., Prem Sai, K., Chandrasekar, B., Gokhale, A. and Basu, S. (2009), “Impact energy absorption of aluminium foam fitted AISI 304L stainless steel tube”, *Mater. Des.*, **30**(5), 1777-1784.
- Seitzberger, M., Rammerstorfer, F.G., Gradinger, R., Degischer, H.P., Blaimschein, M. and Walch, C. (2000), “Experimental studies on the quasi-static axial crushing of steel columns filled with aluminium foam”, *Int. J. Solids Struct.*, **37**(30), 4125-4147.
- Sharifi, S., Shakeri, M., Ebrahimi Fakhari, H. and Bodaghi, M. (2015), “Experimental investigation of bitubular circular energy absorbers under quasi-static axial load”, *Thin-Wall. Struct.*, **89**, 42-53.
- Velmurugan, R. and Muralikannan, R. (2009), “Energy absorption characteristics of annealed steel tubes of various cross sections in static and dynamic loading”, *Latin Am. J. Solids Struct.*, **6**(4), 385-412.
- Yin, H.F., Wen, G.L., Hou, S.J. and Chen, K. (2011), “Crushing analysis and multi objective crashworthiness optimization of honey comb-filled single and bitubular polygonal tubes”, *Mater. Des.*, **32**(8-9), 4449-4460.
- Zhang, Y., Sun, G.Y., Li, G.Y., Luo, Z. and Li, Q. (2012), “Optimization of foam-filled bitubular structures for crashworthiness criteria”, *Mater. Des.*, **38**, 99-109.
- Zhou, Y., Lan, F. and Chen, J. (2011), “Crashworthiness research on S-shaped front rails made of steel–aluminum hybrid materials”, *Thin-Wall. Struct.*, **49**(2), 291-297.

CC